Aeromagnetic noise from magnetometers and data acquisition systems

J. Bradley Nelson, Defence Research & Development Canada - Atlantic, PO Box 1012, Dartmouth, Nova Scotia, Canada B2Y 3Z7

Abstract

Aeromagnetic aircraft and data acquisition systems generate magnetic interference which can effect the quality of the data collected. Many people believe that traditional aircraft compensation, which models the permanent, induced, and eddy-current sources, can remove all of this interference. However, survey aircraft are not perfectly rigid bodies, they have moving ferrous parts, and have changing electrical configurations. In addition, the data acquisition systems can add noise and, as magnetometers become more sensitive, their non-linear behaviour may become important. This paper looks at a variety of noise sources related to the magnetometers and data acquisition systems that do not fit the traditional compensation models, and how they have been dealt with on the National Research Council Convair 580 aircraft.

1. Introduction

"Aircraft compensation" is the term usually applied to the modeling and removal of aircraft-generated magnetic noise due to permanent, induced, and eddy-current sources. These models assume that the airframe is rigid and that there is no hysteresis in the ferrous components of the aircraft. The aircraft-noise model is usually built up from vector magnetometer signals which measure the components of the Earth's magnetic field in the aircraft axes, or from the pitch, roll, and yaw measurements. This "traditional" aircraft compensation is well understood and commercial products are available to perform this noise-removal in real-time. However, both the data acquisition system and cesium magnetometers can produce noise that is not removed by traditional compensation. This paper describes these sources and how they have been dealt with in the NRC Convair 580 aeromagnetics system.

2. Data acquisition system

2.1 Noise generated by the period counting hardware

The most common way to determine the frequency of the Larmor signal, and thus measure the magnetic field, is to time-tag the threshold crossings of the waveform and, by taking the difference between the time-tags, thereby estimate the period (period = 1/frequency). For a typical system, one actually counts the number of threshold crossings (N) during the time between the two time-tags (t_1, t_2) and the magnetic field estimate (B) is given by:

$$\begin{aligned} B \text{ (in nT)} &= \text{Frequency (in Hz)}/3.4986 \\ &= N/[3.4986 \times (t_2 - t_1)] \ . \end{aligned} \quad (1)$$

Two commercial period counting boards have been used on the NRC Convair. The first board, the GT200 made by Guide Technology, has a time-tagging accuracy of 1 ns, and uses two independent time-tags to generate the period measurement. Then there is a small "dead time" during which no time-tags are generated, followed by another pair of time-tags. The user sets a "gate time", which is the time interval over which the board looks for threshold crossings. The second period counting board is the GT654, also made by Guide Technology. This board has a time-tag accuracy of 75 ps, and uses the last time-tag from the initial period estimate as the first time-tag for the next period estimate. Thus there is no dead time. Figure 1 compares the noise spectra of the two period counter boards, when connected to a very-low-noise waveform generator.

Both spectra show discrete frequencies and broad-band features which are related to the waveform generator. They do not coincide because the generator was warming up during the GT200 measurement. However, two features of the GT654 data are immediately apparent. First, the noise floor is curved upward, not flat, because the same time-tag is used in the calculation of two adjacent frequency measurements. If there is a small error in a time-tag, it will produce opposite effects in the two frequency measurements: it will make one slightly too small and the other slightly too large. Therefore the two frequency measurements are not independent as they are in the GT200 board where there was a small dead time between measurements. The second feature is the reduced noise at lower frequencies. This suggests that the data acquisition system noise using the GT654 board will be significantly lower in the 0-15 region Hz than a system using the GT200 board. The Convair data acquisition system uses the GT654 board.

2.2 Counting errors

If there is a small spike or ripple on the Larmor signal very near the point where the signal crosses the threshold, then the board will count an extra threshold crossing. This "counting error" will produce an erroneous period measurement because it will be calculated on N+1, instead of N, threshold crossings. Fortunately, this error leads to a single-data-point glitch in the total-field estimate (see Figure 2), which is easily correctable because Equation (1) can be inverted to determine N.

2.3 Missed samples

If the field being measured is changing at low-frequency, then missing a sample, or repeating the same measurement twice is not a big concern. However, if the field is dominated by a large amplitude, high-frequency, signal, then a missed or repeated sample may lead to a

significant discontinuity. For example if the sampling rate is 160 Hz and the dominant component of the field is a ±50 nT sine wave at 60 Hz, then a missed sample could result in a discontinuity of up to 35.4 nT (worst case as the sine wave passes through zero). After passing through a typical aeromagnetics low-pass filter (~ 1 Hz), this discontinuity would be smeared out over several seconds and would be difficult to remove accurately. Since it is difficult to detect and correct for a missed sample, this provides an upper limit to the sampling rate of the data acquisition system. The GT654 boards used in the Convair system do not miss any samples, even when operated at 200 Hz.

2.4 Noise as a function of sampling rate

Starting with the definition of the measured period leads to

$$\sigma_T = \sigma_t/N \ , \qquad (2)$$

where σ_T is the standard deviation of the period measurements and σ_t is the standard deviation of the individual time tags. The frequency measurements are related to the period measurements by the relation

$$F=1/T \quad , \text{so} \qquad (3)$$

$$\sigma_F = (1/T_o^2)\sigma_T = \sigma_t F_o^2/N \qquad (4)$$

where T_o and F_o are the average period and frequency (related to the ambient magnetic field by Equation (1)). The relationship between the sampling rate (S) and the number of threshold crossings (N) is

$$N = F_o/S \ . \qquad (5)$$

For example, if the average magnetic field was 45,732.58 nT, then the Larmor frequency would be 160,000 Hz. If the sampling rate was 160 Hz, then there would be N=1000 threshold crossings during that measurement. Substituting Equation (5) into (4) and converting σ_F into σ_B via Equation (1) gives

$$\sigma_B = \sigma_t F_o S/3.4986 \ . \qquad (6)$$

Finally, the normalized noise is obtained by dividing σ_B by the square root of the bandwidth, which is just the sampling rate divided by two.

$$\text{Normalized Noise} = \sigma_B/\sqrt{\text{Bandwidth}} = (1/3.4986) \times \sqrt{2} \times \sigma_t \times F_o \times \sqrt{S} \ . \qquad (7)$$

Equation (7) indicates the normalized noise floor should increase as the square root of the sampling rate. Figure 3 shows the measured white noise floor vs square root of sampling rate for a Scintrex Ltd. CS-2 magnetometer mounted inside a Mu-metal shield. The measurements were performed with the GT200 board. Clearly the data are consistent with Equation (7). Thus it is not a good idea to use an extremely-high sample rate magnetic data acquisition system. However, in order to determine which sampling rate is best, it is necessary to know if magnetic noise exists at higher frequencies and if so, then the frequencies at which this occurs.

3. Magnetometer noise sources
3.1 Tumble and spin errors

All optically-pumped magnetometers have an orientation dependence - that is, they will give slightly different readings if the optical axis of the sensor is tilted with respect to the Earth's field (tumble) or if the sensor is rotated about the optical axis (spin). In the case of oriented magnetometers which are used by most military organizations, this effect is negligible because servo mechanisms maintain the sensor in the optimum orientation. For strapdown magnetometers though, the effect is significant.

Spin curves for magnetometers usually show a sinusoid with ~ 1 nT maximum error. The source of this spin error is usually magnetic contamination in the construction of the magnetometer. Fortunately, this error is very well characterized by the standard aircraft compensation model and so is not a concern.

A typical tumble curve is shown in Figure 4. There is only a small orientation effect as long as the magnetometer is not operated near the "dead zones" near 90°, 180°, 270°, and 360°. Previous attempts to measure the angle between the optical axis and the Earth's field, and use that parameter as an extra term in the aircraft compensation model, have not led to improved compensation (Hardwick, 2003). This is because the extra term is mathematically very similar to a linear combination of terms in the standard model. However, the best way to avoid tumble and spin noise to ensure that the optical components inside the magnetometer are properly aligned, and not to bank too close to a dead zone angles.

3.2 Heater current noise

In addition to magnetometer self-noise, there is the possibility of temperature-dependent noise from the heater circuit. Even though this heater typically runs at 5-10 kHz, these small signals can effect the threshold crossings. If the heater frequency is stable, then it would create a discrete frequency in the PSD of the magnetometer output. However, very little care is taken by commercial magnetometer manufacturers to stabilize the heater circuitry temperature (Mihajlovic, 2001; Smith, 2001). Thus the heater modulation tends to drift with temperature and may occasionally alias into the frequency band of interest. The noise has a distinctive "swept frequency" appearance as seen in Figure 5, taken from Nelson 1999. CS-2 magnetometers which employ separate the power and signal cables are used on the NRC Convair to avoid this problem. Alternatively, the Larmor signal can be band-pass filtered to remove the heater modulation.

3.3 DC shifts due to magnetometer non-linearity

The non-linearity of a typical cesium magnetometer is shown in Figure 6 (Onno). Notice that the non-linearity is

asymmetric; if an AC magnetic field is picked up by the magnetometer, it will lead to a slight error in the average field detected. Figure 7 illustrates the DC shift caused by this non-linearity as a function of AC signal amplitude for a typical cesium magnetometer. Clearly there is only a tiny DC shift unless the AC signal amplitude is hundreds of nT. However, as the aircraft manoeuvres, the DC shift will be modulated and, if there is a very large AC noise source present, it could lead to extra low-frequency noise related to the manoeuvres.

3.4 Shifts due to vector addition of DC and AC fields

Assume that the magnetic field vector consists of a DC background field (B) and an alternating component ($A\sin(\omega t)$). The angle of the alternating field vector can have any value with respect to the DC background field vector as shown in Figure 8 (reproduced from Onno).

If the two vectors are exactly in line, the resulting average value of the total field vector is clearly just B. For all other angles though, the average will be slightly more than B. Figure 9 illustrates the DC shift caused by the vector addition of a 50,000 nT background (DC) field and an AC field at right angles to it. Clearly the DC shift is only a few pT unless the AC field is greater than 50 nT.

This derivation concentrated on the DC shift caused by the vector addition of the background and alternating fields but, as the aircraft manoeuvres, the AC field vector will change orientation with respect to the background (DC) field vector. Thus the DC shift shown in Figure 9 will be modulated in some way by the aircraft heading and attitude and, in the same way as the non-linearity of the magnetometer, could lead to low-frequency noise. In the Convair, the AC fields have been measured at only a few nT so neither of these sources is a problem.

4. Conclusions

This paper has described a number of magnetic noise mechanisms related to the data acquisition system and magnetometers that are not modeled and removed by standard aircraft compensation algorithms. For the specific case of the NRC Convair, the Guide Technology GT654 board was chosen because it has lower overall noise in the band of interest (0-15 Hz). The curved noise floor is not a problem for our purposes and we have implemented a real-time "counting error" detection and correction algorithm. The sampling rate was chosen to be 160 Hz because there were no missed samples, the board noise is still well below the magnetometer white noise, and no other spectral features aliased back into the band of interest (not described in this paper). Tumble and spin errors are not a problem as long as the optical components in the magnetometers remain aligned, and the heater current does not couple back into the field measurements on CS-2 magnetometers when the TTL output is used. The AC fields in the aircraft during flight have been measured at only a few nT peak-to-peak so the magnetometer non-linearity and vector addition of AC and DC fields are not concerns.

8. References

Hardwick, C.D., Hardwick Consulting, Ottawa Ontario. Personal Communication.

Mihajlovic, George, Scintrex Ltd., Mississauga, Ontario. Personal Communication, 2001

Nelson, J. Bradley, "Performance of the Magnetic Data Acquisition System (MAGDAS) During the Naval Research Laboratory '99 Arctic Aeromagnetic Survey", NRC LTR-FR-157, August 1999.

Onno, T., "Development of a High Performance Airborne Magnetometer Data Acquisition System", unpublished manuscript.

Smith, Ken, Geometrics Ltd., Sunnyvale California. Personal Communication, 2001

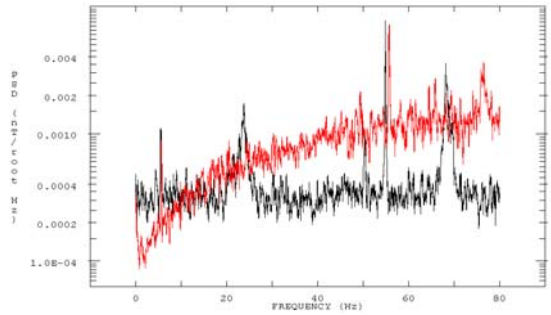

Figure 1. PSD of the synthesizer signal, measured at two different times, with theGT200 board (black) and the GT654 board (red).

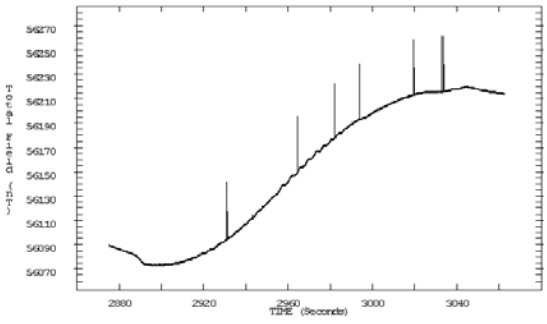

Figure 2. Counting error glitches seen in Convair flight data (SR=160 Hz).

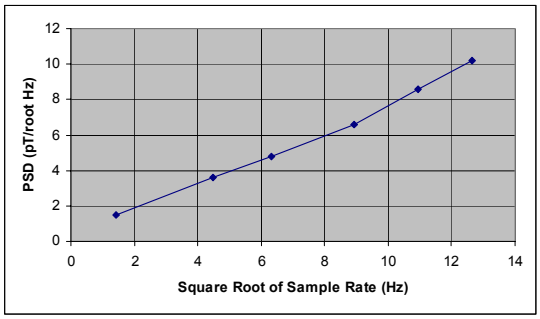

Figure 3. White noise as a function of square root of sampling rate with the GT200 board.

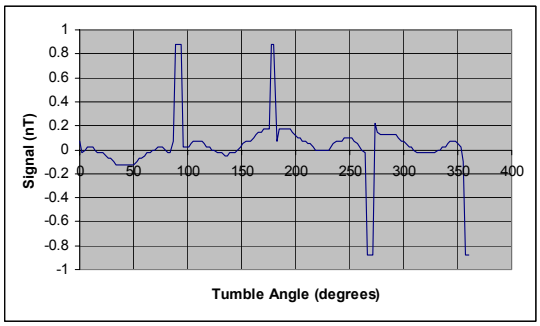

Figure 4. Tumble curve for a CS-2 magnetometer.

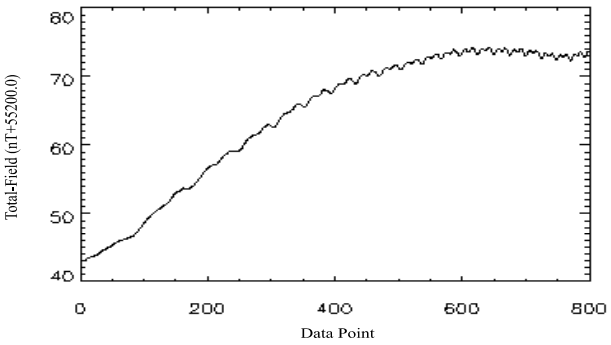

Figure 5. “Swept frequency” heater current noise.

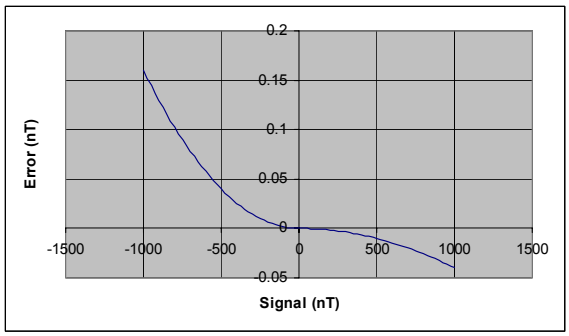

Figure 6. Non-linearity of a typical cesium magnetometer.

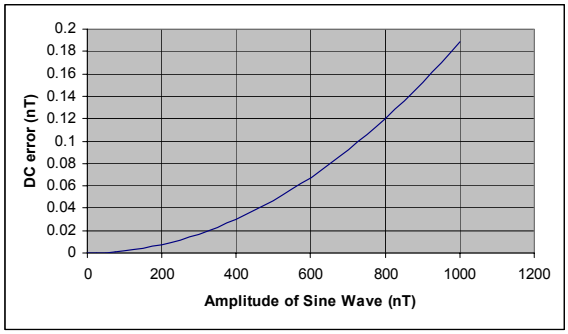

Figure 7. DC shift caused by magnetometer non-linearity as a function of AC signal amplitude.

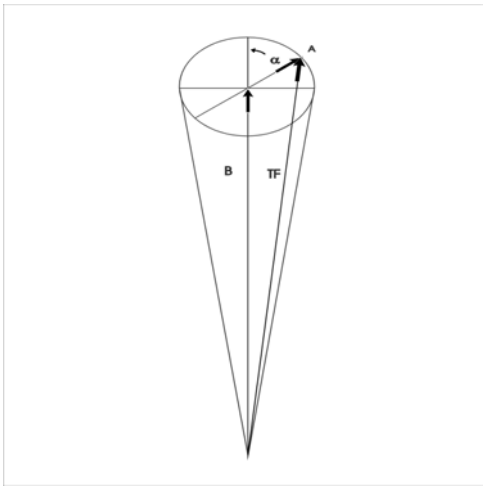

Figure 8. Vector addition of DC and AC fields.

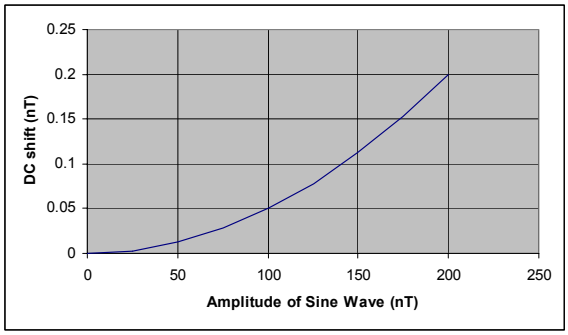

Figure 9. DC shift caused by vector addition of 50,000 nT DC background field and AC field at right angles to it.